0026-895X/98/020304-09$3.00/0

MOLECULAR PHARMACOLOGY, **53:**304–312 (1998).

M_2 Receptor Binding of the Selective Antagonist AF-DX 384: Possible Involvement of the Common Allosteric Site

C. TRÄNKLE, I. ANDRESEN, G. LAMBRECHT, and K. MOHR

Department of Pharmacology and Toxicology, Institute of Pharmacy, University of Bonn, 53121 Bonn, Germany (C.T., K.M.), Department of Pharmacology, University of Kiel, Hospitalstraße 4, 24105 Kiel, Germany (I.A.), and Department of Pharmacology, Biocenter Niederursel, University of Frankfurt, 60439 Frankfurt/Main, Germany (G.L.)

Received August 6, 1997; Accepted October 24, 1997

This paper is available online at http://www.molpharm.org

ABSTRACT

The hypothesis was tested that M_2-selective antagonists partially utilize the allosteric site of muscarinic M_2 receptors. The interactions of the allosteric agent W84 (hexane-1,6-bis[dimethyl-3′-phthalimidopropyl-ammonium bromide]) were studied with the M_2/M_4-selective AF-DX 384 [(±)-5,11-dihydro-11-{[(2-{2-[(dipropylamino)methyl]-1-piperidinyl}ethyl)amino]carbonyl}-6*H*-pyrido(2,3-*b*)(1,4)-benzodiazepine-6-one], the nonselective *N*-methylscopolamine (NMS), and a number of other muscarinic antagonists. In isolated paced guinea pig atria, the antagonistic effect of W84 against oxotremorine- and arecaidine propargyl ester-induced negative inotropic actions reached a limiting value at higher W84 concentrations, revealing negative cooperativity (factors of cooperativity $\alpha = 311$ and $\alpha = 495$, respectively). The antagonistic potency of W84 in this M_2 receptor model (W84 binding constant $K_A \sim 160$ nM) was higher than at M_1/M_4-like receptors of rabbit vas deferens ($K_B \sim 800$ nM) and at M_3 receptors of guinea pig ileum ($K_B \sim 4{,}000$ nM). In paced atria, combinations of W84 with muscarinic antagonists yielded more-than-additive antagonistic effects against oxotremorine in case of conventional antagonists such as NMS ($\alpha = 18$) but less-than-additive effects with the M_2-preferring AF-DX 384 ($\alpha = 444$). In guinea pig heart homogenates, the equilibrium binding of [^{3}H]NMS was only partially inhibited by W84 ($\alpha = 2.4$), whereas [^{3}H]AF-DX 384 binding could be suppressed completely ($\alpha = 194$). The difference in cooperativity reflects that W84 inhibits [^{3}H]NMS dissociation with a ~40-fold higher potency ($EC_{diss} = 900$ nM) than [^{3}H]AF-DX 384 dissociation ($EC_{diss} = 33{,}300$ nM). [^{3}H]NMS dissociation also could be retarded by AF-DX 384 ($EC_{diss} = 22{,}000$ nM), probably via an interaction with the site used by W84. The results suggest that the binding domain of AF-DX 384 partially overlaps with the common allosteric site of the M_2 receptor protein.

Conventional muscarinic antagonists are not subtype selective. The orthosteric antagonist binding site seems highly conserved among the five muscarinic receptor subtypes. The orthosteric site is thought to be located within a ligand binding pocket formed by the transmembranous helices (Wheatley *et al.*, 1988; Trumpp-Kallmeyer *et al.*, 1992; Wess, 1993).

M_2-selective antagonists utilize different points of attachment on M_2 receptors (Birdsall *et al.*, 1989). It has been suggested that extramembranous receptor domains may be involved in the subtype-selective binding of M_2 antagonists (Melchiorre *et al.*, 1989; Pedder *et al.*, 1991; Wess *et al.*, 1992; Kerckhoff and Höltje, 1994).

Allosteric modulators of ligand binding to muscarinic receptors generally have a high affinity to M_2 receptors (Ellis *et al.*, 1991; Lee and El-Fakahany, 1991; Jakubík *et al.*, 1995). These drugs are capable of binding to muscarinic receptors even if the orthosteric site is occupied by a ligand such as the antagonist NMS. As a consequence, the dissociation of the orthosteric ligand is altered by the allosteric modulator; commonly, ligand dissociation is retarded. When the allosteric modulator has bound to the free receptor, the association of the ligand is impaired. The effect of an allosteric modulator on the equilibrium binding of the ligand depends on the balance between the actions on ligand association and dissociation (Kostenis and Mohr, 1996). Functionally, the known allosteric modulators behave as antagonists. Results of biochemical (Pedder *et al.*, 1991), mutagenesis (Ellis *et al.*, 1993; Leppik *et al.*, 1994), and chemical modification (Jakubík and Tuček, 1995) studies suggest that allosteric modulators bind at the entrance of the ligand binding pocket of the M_2 receptor.

Because M_2-selective antagonists and allosteric modulators share a similar subtype-selectivity pattern and are likely to interact with the receptor at the entrance of the ligand binding pocket, the question arises whether M_2-selective antagonists may use points of attachment that are part of the

This work was supported by the Deutsche Forschungsgemeinschaft (K.M.) and the Fonds der Chemischen Industrie (G.L.).

ABBREVIATIONS: NMS, *N*-methylscopolamine; APE, arecaidine propargyl ester; NBS, (−)-*N*-butylscopolamine; W84, hexane-1,6-bis(dimethyl-3′-phthalimidopropyl-ammonium bromide); DR, dose ratio; 4-Cl-McN-A-343, 4-(4-chlorophenylcarbamoyloxy)-2-butynyltrimethylammonium iodide.

common allosteric site (Ellis and Seidenberg, 1992) of muscarinic M_2 receptors.

To check for such an interplay, we investigated in functional and radioligand binding experiments the interaction between the allosteric model compound W84 (Fig. 1) and the M_2/M_4-selective antagonist AF-DX 384 [(±)-5,11-dihydro-11-{[(2{2-[(dipropylamino)methyl]-1-piperidinyl}ethyl)amino]carbonyl}-6*H*-pyrido(2,3-*b*)(1,4)benzodiazepine-6-one] (Fig. 1). For the sake of comparison, the nonselective antagonist NMS was included with a number of structurally related and unrelated antagonists. W84 was chosen as allosteric model compound because, first, it has been shown to interact with the common allosteric site on the M_2 receptor protein (Tränkle and Mohr, 1997). Second, W84 has a rather high affinity to the allosteric site in antagonist M_2 receptor complexes even under organ bath conditions (Jepsen *et al.*, 1988; Lüß and Mohr, 1992). Third, structure-activity relationships for the stabilizing effect of W84 on NMS-occupied M_2 receptors have been characterized (Kostenis *et al.*, 1994). Forth, in isolated beating guinea pig atria, combinations of W84 with atropine (Lüllmann *et al.*, 1969) and NMS (Maaβ *et al.*, 1995) have been shown to induce more-than-additive antimuscarinic effects.

AF-DX 384 was chosen as a representative M_2-preferring antagonist (Miller *et al.*, 1991) because it is available in a radiolabeled form, allowing for direct binding studies.

The test compounds were applied in isolated beating guinea pig left atria to study interactions under "physiological conditions" as well as in radioligand binding experiments with guinea pig cardiac membranes to gain a more direct insight into the events on the molecular level.

Materials and Methods

Experiments in Isolated Organs

Preparation of guinea pig left atria was carried out as described previously (Maaß *et al.*, 1995). The atria were mounted in 20-ml organ baths filled with Tyrode's solution (149.2 mM Na^+, 2.7 mM K^+, 1.8 mM Ca^{2+}, 1.1 mM Mg^{2+}, 145.5 mM Cl^-, 12.0 mM HCO_3^-, 0.2 mM $H_2PO_4^-$, 5.5 mM glucose, pH 7.3), which was maintained at 32° and oxygenated with 95% O_2/5% CO_2. Atria were preloaded with 10 mN and electrically stimulated via platinum contact electrodes with rectangular pulses of 5-msec duration at a frequency of 3 Hz. Isometric force of contraction after an initial equilibration period of 60-min duration in the absence of any drug was set at 100%. Cumulative concentration-effect curves for the negative inotropic effect of oxotremorine were recorded with each concentration present for 10 min. The oxotremorine concentration at which the force of contraction was reduced by 50% was used as a measure of potency (EC_{50}). After a wash-out period of 30 min, including three changes of the incubation medium after 0, 10, and 20 min, the atria were incubated with an antagonistic test compound for 60 min before the next concentration-effect curve of oxotremorine was recorded. After another washing period of 30 min to remove the agonist, a combination of the antagonistic test compound and another antagonist of interest was applied for 60 min, and the concentration-effect curve of oxotremorine was determined again. Control experiments revealed that the order in which W84 and the respective antagonists were applied did not influence the effect of the combination. To characterize the concentration dependency of the antioxotremorine effect of a test compound, the same schedule was applied except a higher concentration of antagonist was applied instead of a combination.

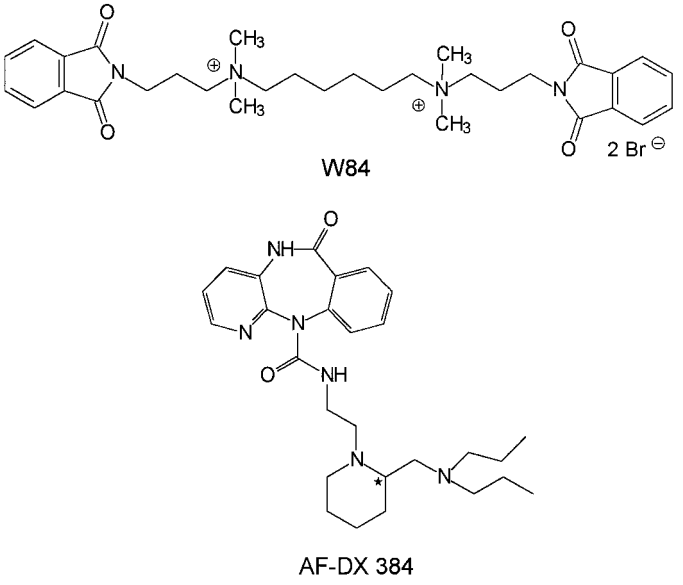

Fig. 1. Structural formulas of the allosteric modulator W84 and the M_2/M_4-selective antagonist AF-DX 384. *, center of chirality.

A set of experiments was carried out to investigate the muscarinic receptor subtype selectivity of W84; thus, the pharmacological properties of W84 were examined at prejunctional muscarinic heteroreceptors in rabbit vas deferens (M_1/M_4-like receptors; 4-Cl-McN-A-343 as agonist) and in guinea pig atria (M_2 receptors; APE as agonist) and ileal longitudinal smooth muscle (M_3 receptors; APE as agonist). Tissues were isolated from adult guinea pigs of either sex or from male New Zealand White rabbits previously killed by cervical dislocation or intravenous injection of 120 mg/kg pentobarbitone sodium, respectively. The methods used have been described in detail previously (Waelbroeck *et al.*, 1994, 1996).

Binding Studies

Preparation of guinea pig cardiac membranes. Cardiac membranes were prepared as described previously at an ambient temperature of 3–6° (Jepsen *et al.*, 1988). Briefly, pieces of ventricular myocardium of guinea pig hearts were homogenized in a 0.32 M sucrose solution. The homogenate was centrifuged for 10 min at 2,500 × *g* (5,000 rpm in a Beckman rotor 21; Beckman Instruments, Columbia, MD). The supernatant was centrifuged for 30 min at 77,200 × *g* (31,500 rpm in a Beckman rotor 35). The resulting pellet was resuspended in 50 mM Tris·HCl, pH 7.4. Aliquots of 1 ml were frozen in liquid nitrogen and stored at −80°. Protein content amounted to 4.9–7.3 mg/ml membrane suspension.

Binding assays. [^{3}H]NMS and [^{3}H]AF-DX 384 had specific activities of 85.1 and 90.4 Ci/mmol, respectively. Cardiac membranes at a protein concentration of 300–400 μg/ml were incubated with either 0.5 nM [^{3}H]NMS or 2 nM [^{3}H]AF-DX 384 in a final volume of 1.5 ml. Experiments were performed in a buffer composed of 50 mM Tris·HCl, and 3 mM $MgHPO_4$, pH 7.3, at 23°. Nonspecific ^{3}H-radioligand binding was determined in the presence of 100 μM atropine and did not exceed 10% of [^{3}H]NMS total binding or 25% of [^{3}H]AF-DX 384 total binding. The binding characteristics of [^{3}H]NMS and [^{3}H]AF-DX 384 under control conditions were investigated in homologous competition experiments with 2 hr of incubation. The K_D and B_{max} values were 0.9 nM and 233 fmol/mg of protein for [^{3}H]NMS binding and 11 nM and 320 fmol/mg of protein for [^{3}H]AF-DX 384 binding. These results are in good agreement with the K_D value of 8.7 nM reported by Entzeroth and Mayer (1990) in rat cardiac homogenates for [^{3}H]AF-DX 384 binding. The effect of increasing concentrations of W84 on radioligand equilibrium binding was measured with 2 nM [^{3}H]AF-DX 384 after 3 hr of incubation and with 0.2 nM [^{3}H]NMS after 4 hr of incubation.

To measure drug effects on the dissociation of [^{3}H]NMS or [^{3}H]AF-DX 384, the respective radioligand and membranes were incubated for 120 min before the dissociation was revealed by the addition of

100 μM atropine alone or in combination with the indicated test compound. Radioligand dissociation was observed generally over 120 min. When [^{3}H]NMS dissociation was measured in the presence of combinations of AF-DX 384 and W84, the observation period was extended to 4 hr. Membranes were separated by rapid filtration (glass fiber filters No. 6; Schleicher & Schüll, Dassel, Germany). Filters were washed twice with 5 ml of ice-cold incubation buffer, dried, and placed into scintillation vials containing 5 ml of Ready Protein (Beckman) before the filter-bound radioactivity was determined by liquid scintillation counting.

Data Analysis

Experiments with isolated organs. Agonist concentration-effect curves were fitted by nonlinear regression analysis using the general Hill equation, and the concentration for a half-maximum effect was determined (EC_{50}). DRs served to quantify antagonist-induced curve shifts: $DR = EC_{50,test\ compound}/EC_{50,control}$. The concentration dependency of the effect of a given antagonist was analyzed according to Arunlakshana and Schild (1959) or Lanzafame *et al.* (1996). The latter analysis is appropriate to describe antagonistic effects in terms of the ternary allosteric model of Ehlert (1988) and is based on the equation:

$$DR - 1 = \frac{(\alpha - 1)}{(\alpha \cdot K_A/[A] + 1)} \quad (1)$$

where [A] is the concentration of the allosteric modulator, K_A is the equilibrium dissociation constant of the modulator, and α is the cooperativity factor for the interaction of the modulator with the respective agonist.

The expected DR (DR_{exp}) for a combination of antagonists can be calculated as $DR_{exp} = DR_{ant1} + DR_{ant2} - 1$, if the interaction is competitive (Lüllmann *et al.*, 1969; Clark and Mitchelson, 1976). More-than-additive or less-than-additive effects as observed with W84 in combinations with the antagonists were analyzed according to Christopoulos and Mitchelson (1994) using the equation:

$$DR_{AB} = \frac{\alpha \cdot K_A}{\alpha \cdot K_A + [A]}\left(1 + \frac{[B]}{K_B} + \frac{[A]}{K_A} + \frac{[A] \cdot [B]}{\alpha' \cdot K_A \cdot K_B}\right) \quad (2)$$

where K_A and K_B denote the equilibrium dissociation constants of the allosteric modulator and orthosteric antagonist, respectively, at the free receptor, and the cooperativity factors α and α' describe the interaction of the allosteric modulator A with the agonist and the antagonist B, respectively. The equation was rearranged to obtain α' for the interaction of W84 and the respective antagonist.

Binding data. Experimental results were analyzed by computer-aided, nonlinear regression analysis using Prism Version 2.01 (GraphPAD Software, San Diego, CA). Curve fitting to competition data was based on the general Hill equation. Because the observed Hill coefficients in homologous competition experiments did not differ significantly from unity (partial F test, $p > 0.05$, data not shown), IC_{50} values were determined from curve fits with n_H fixed to 1. K_D and B_{max} values were calculated from these IC_{50} values according to DeBlasi *et al.* (1989).

The inhibition curves for the effect of W84 on the binding of [^{3}H]AF-DX 384 and [^{3}H]NMS, respectively, were analyzed according to Ehlert (1988) using the equation:

$$B = B_0 \frac{(L + K_D)}{\left\{L + K_D \cdot \frac{(K_A + A)}{(K_A + A/\alpha)}\right\}} \quad (3)$$

where B_0 denotes the equilibrium binding of a fixed radioligand concentration in the absence of allosteric ligand A, K_D is the equilibrium dissociation constant of the radioligand, K_A is the equilibrium dissociation constant of the allosteric ligand at the free receptor, and α is the cooperativity factor for the interaction between the allosteric modulator and the radioligand.

Dissociation data were fitted using a monoexponential decay function that yielded the apparent rate constant of dissociation, k_{-1}. Curve fitting to obtain concentration-effect curves for the retardation of radioligand dissociation was based on a four-parameter logistic function.

The antagonistic action of AF-DX 384 on the W84-induced retardation of [^{3}H]NMS dissociation was analyzed according to a method described by Lazareno and Birdsall (1993). The procedure can be regarded as a condensed form of the Schild method (Arunlakshana and Schild, 1959) to analyze the action of an antagonist. The approach is based on the simultaneous analysis of the concentration-effect curve of an effector agent E determined in the absence of antagonist and of the antagonist concentration-effect curve for the attenuation of the action of a single, fixed effector concentration. Here, the observed effect was the retardation of [^{3}H]NMS dissociation by W84 in the absence and presence of AF-DX 384. To reveal the antagonistic action of AF-DX 384, its own effect on [^{3}H]NMS dissociation was eliminated from the analysis by normalization (for details, see Results). The W84 and AF-DX 384 curves were fitted nonlinearly using as two independent variables the concentrations of W84 and AF-DX 384, respectively. This analysis was based on the following equation (Lazareno and Birdsall, 1993) with application of SigmaPlot for Windows (version 3.03; Jandel Scientific Software, San Rafael, CA):

$$\text{Effect} = \frac{(E_{max} - \text{basal})}{\left(1 + \left\{EC_{50}{}^0 \cdot \left(\frac{[B]^s}{K_B} + 1\right)/[E]\right\}^n\right)} + \text{basal} \quad (4)$$

where E_{max} and basal denote the maximum and minimum effect level of the effector, respectively, [E] is the concentration of the effector, n is the slope of the effector curve. EC_{50} indicates the concentration at which the effector produces a half-maximal effect, [B] is the concentration of the antagonist, K_B denotes the equilibrium dissociation constant of the antagonist, and s is the Schild factor.

Drugs

[^{3}H]NMS and [^{3}H]AF-DX 384 were purchased from New England Nuclear-Dupont (Bad Homburg, Germany). Oxotremorine sesquifumarate, atropine sulfate, (−)-scopolamine hydrobromide, (−)-scopolamine methylbromide, and (−)-scopolamine *N*-butylbromide were from Sigma Chemical (München, Germany). (+)-Dexetimide hydrochloride was from ICN Biomedicals (Meckenheim, Germany). Methoctramine tetrahydrochloride was from Research Biochemicals International (Natick, MA). AF-DX 384 was generously provided by Dr. Karl Thomae GmbH (Biberach an der Riβ, Germany). W84 was synthesized by Dr. Joachim Pfeffer (University of Kiel, Germany) according to Wassermann (1970). APE and 4-Cl-McN-A-343 were synthesized by Dr. Ulrich Moser (University of Frankfurt, Germany) according to Waelbroeck *et al.* (1994).

Results

In paced guinea pig atria, all test compounds antagonized the negative inotropic effect of the agonist oxotremorine. The concentration-effect curves of oxotremorine ($-\log EC_{50}$ = 7.89 ± 0.03, mean ± standard error, 184 experiments) were shifted by the test compounds in a parallel fashion to higher concentrations; the extent of rightward shift was expressed as DR. In Fig. 2, the DRs thus obtained for various concentrations of NMS, AF-DX 384, and W84, respectively, are plotted according to Arunlakshana and Schild (1959). For NMS and AF-DX 384, the data points could be fitted by lines with a slope of unity, as to be expected for a competitive interplay with the agonist. As a measure for the affinity to

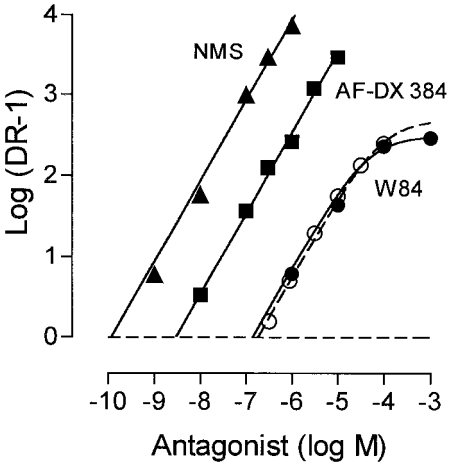

Fig. 2. Antagonistic action of the indicated compounds at muscarinic M_2 receptors in isolated paced guinea pig left atria. The antagonist-induced rightward shift of the concentration-effect curves for the negative inotropic action of the agonists oxotremorine (▲, ■, ●) and arecaidine propargyl ester (○) is quantified as DR = $EC_{50,\ antagonist}/EC_{50,\ control}$ and displayed in a Schild plot. Results are mean values from four or five experiments in separate atrial preparations. For the antagonists NMS and AF-DX 384, the points could be connected by linear regression lines with slopes not significantly different from unity ($p > 0.05$, t test). In case of W84, the curves were fitted by nonlinear regression analysis based on the ternary complex model of allosteric interactions.

the M_2 receptor, the pK_B values (i.e., the concentrations at log [(DR − 1) = 0), are indicated in Table 1. In case of W84, the antagonistic action against oxotremorine saturated at higher concentrations. According to the allosteric model, a curvilinear Schild plot reaching a limiting value at high concentrations of antagonist indicates allosteric modulation of agonist binding in a negative cooperative fashion (Ehlert, 1988). Thus, the data analysis was based on the allosteric model (Ehlert, 1988; Lanzafame *et al.*, 1996). At log (DR − 1) = 0, the allosteric fit yields, corresponding to a Schild analysis for a competitive interaction, an estimate of the equilibrium dissociation constant K_A for the binding of W84 at the free receptor. The limiting value reached by the curved line at higher concentrations of W84 is a measure of the degree of negative cooperativity between the allosteric ligand acting at a site different from the agonist binding site and the agonist at its binding site (Lanzafame *et al.*, 1996). Table 2 indicates the binding constant K_A of W84 for the free M_2 receptor and the cooperativity factor α for the interaction between W84 and oxotremorine. The findings made in guinea pig atria with the muscarinic agonist arecaidine propargyl ester [−log EC_{50} = 8.07 ± 0.04 (mean ± standard error), 18 experiments] in the set of experiments to check for an M_2 selectivity of W84 are included in Fig. 2 and Table 2. In addition, with this agonist, the curvilinear fit was significantly better than a linear fit (partial F test, $p < 0.05$). As expected, the K_A value of W84 was independent of the agonist applied (t test, $p > 0.05$). The cooperativity factor α (Table 2) did not differ significantly (t test, $p > 0.05$) for either oxotremorine or APE as the agonist.

Electrical field stimulation of the rabbit vas deferens (M_1/M_4-like receptors) elicited neurogenic twitch contractions that could be concentration-dependently inhibited by the M_1-selective muscarinic receptor agonist 4-Cl-McN-A-343 [−log EC_{50} = 6.89 ± 0.05 (mean ± standard error), 12 experiments]. Isotonic contractions of guinea pig ileum (M_3 receptors) were induced by cumulative addition of APE [−log EC_{50} = 7.67 ± 0.04 (mean ± standard error), 9 experiments]. In both tissues, W84 surmountably antagonized the responses to the agonists. There was a concentration-dependent parallel shift to the right of agonist concentration-response curves without either the basal tension or maximal effects being affected. The Schild plots were linear throughout the antag-

TABLE 1

Antagonistic effects against the negative inotropic action of oxotremorine in isolated paced guinea pig left atria as induced by the indicated antagonists and by W84, as well as by combinations of W84 with the antagonists

pK_B-values, presented as mean ± standard error, denote the respective dissociation constants for the antagonists at the cardiac muscarinic receptor derived from Schild analyses (Arunlakshana and Schild, 1959) as illustrated in Fig. 2 for NMS and AF-DX 384. DR_{ant} and DR_{W84} quantify the rightward shift of the oxotremorine concentration-effect-curve as induced at the indicated concentrations by the antagonists and by W84, respectively. DR_{exp} is the oxotremorine curve shift to be expected if two competitive antagonists were combined. DR_{obs} indicates the experimentally observed shift induced by the combination of antagonist plus W84. F = DR_{obs}/DR_{exp} and indicates the deviation of the observed antagonistic effect from the expected effect. α is the cooperativity factor for the interaction of W84 with the respective orthosteric antagonist according to the cooperativity model. Given are means ± standard error of four to six experiments in separate atria.

Antagonist	pK_B	Antagonist concentration	DR_{ant}	W84 concentration	DR_{W84}	DR_{exp}	DR_{abs}	F	α	Mean α
		μM		μM						
AF-DX 384	8.5 ± 0.03	3		100	254 ± 45	1,477	1,162 ± 81	0.8	338	
			1,224 ± 120							444
		3		1,000	350 ± 51	1,573	882 ± 91	0.6	550	
Dexetimide	9.8 ± 0.17	0.3		100	223 ± 82	971	4,556 ± 1,301	4.7	109	
			749 ± 94							92
		0.3		1,000	211 ± 8	959	7,980 ± 1,751	8.3	74	
Atropine	9.1 ± 0.05	1	992 ± 169	100	295 ± 33	2,235	11,094 ± 1,433	5.0	26	
										19
		1	1,796 ± 302	1,000	269 ± 15	2,647	30,622 ± 3,908	11.6	12	
(−)-Scopolamine	9.1 ± 0.02	0.3	372 ± 13	100	219 ± 18	590	3,634 ± 364	6.2	25	
										37
		0.3	306 ± 30	1,000	197 ± 25	502	2,651 ± 393	5.3	48	
(−)-NMS	9.9 ± 0.07	0.1	1,064 ± 93	100	335 ± 85	1,398	8,133 ± 1,840	5.8	13	
										18
		0.1	1,164 ± 123	1,000	195 ± 11	1,358	18,238 ± 3,226	13.4	23	
(−)-NBS	7.2 ± 0.08	30	499 ± 27	100	234 ± 18	732	4,082 ± 56	5.6	28	
										33
		30	332 ± 55	1,000	204 ± 5	535	4,135 ± 368	7.7	37	
Methoctramine	7.9 ± 0.04	3	198 ± 32	1,000	226 ± 28	423	217 ± 20	0.5	N.D.	

N.D., Not determinable; the experimental data set yielded a negative value for α.

TABLE 2

Antagonistic action of W84 at M_1/M_4-like receptors in rabbit vas deferens (RDV), at M_2 receptors in guinea-pig atria (GPA), and at M_3 receptors in guinea-pig ileum (GPI)

The equilibrium dissociation constants K_A and cooperativity factors α for the allosteric interaction of W84 with oxotremorine (Oxo) and APE, respectively, at M_2 receptors were derived from an analysis based on the cooperativity model. The interaction of W84 with 4-Cl-McN-A-343 (McN) at M_1/M_4 and APE at M_3 receptors was analysed according to Arunlakshana and Schild (1959). Because the slopes of the Schild plots did not differ significantly ($p > 0.05$, t test) from unity, K_B values were estimated by fitting to the data the best straight line with a slope of 1.00. Listed are mean values ± standard error of three to eight experiments performed in separate preparations.

Subtype	Agonist	Cooperativity model		Competitive model	
		K_A	α	K_B (Constrained plot)	Slope
		nM		*nM*	
M_1/M_4 (RDV)	McN	N.D.	N.D.	759 ± 67	1.15 ± 0.06
M_2 (GPA)	Oxo	137 ± 28	311 ± 16	N.D.	N.D.
	APE	180 ± 11	495 ± 108	N.D.	N.D.
M_3 (GPI)	APE	N.D.	N.D.	4,370 ± 820	1.21 ± 0.23

N.D., not determined.

onist concentration range studied (vas deferens: 1, 3, 10, and 30 μM; ileum: 10, 30, and 100 μM), and the slopes were not significantly different from unity (t test, $p > 0.05$) (Table 2). Thus, W84 was an apparently simple competitive antagonist in the two preparations studied, with K_B values of 759 and 4370 nM in vas deferens and ileum, respectively (Table 2). These results show that W84 exhibits a higher antimuscarinic potency at atrial M_2 receptors (K_A ~160 nM, Table 2) than at the other muscarinic receptor subtypes. It possesses the following selectivity profile: $M_2 > M_1/M_4 > M_3$ (Table 2). This profile of W84 is similar to that of two other allosteric modulators, gallamine (Ellis *et al.*, 1991) and alcuronium (Jakubík *et al.*, 1995).

The interaction of W84 with AF-DX 384 and other antimuscarinic drugs was studied in guinea pig atria with oxotremorine as the agonist. First, the antagonistic effect of the antimuscarinic drugs alone was measured at various drug concentrations. As expected for competitive antagonists, linear Schild plots with slopes not significantly different from unity were obtained (data not shown). The respective pK_B values are listed in Table 1. In the combination experiments with W84, the competitive antagonists were applied at selected concentrations that induced a rightward shift (DR_{ant}) of the oxotremorine control curve by factors of 200-1800 (Table 1). The antagonists were combined with 100 and 1000 μM W84 (except for methoctramine, which was applied only in the presence of 1000 μM W84). The DRs induced by W84 alone in the respective sets of experiments are indicated in Table 1. The overall mean ± standard error values amounted to $DR_{W84} = 260 \pm 19$ at 100 μM W84 and $DR_{W84} = 236 \pm 21$ at 1000 μM W84 (Table 1). The antimuscarinic effects found in the combination experiments with 1000 μM W84 are displayed in Fig. 3. All combinations with W84 except that of AF-DX 384 and methoctramine elicited a higher degree of antagonism than expected for a combination of two competitive antagonists. The extent of the deviation from competitive behavior was quantified by the factor $F = DR_{obs}/DR_{exp}$ (Table 1). Combined with conventional antagonists, W84 induced F values of >1, indicating more-than-additive effects (Table 1). In contrast, less-than-additive effects ($F < 1$) were found when W84 was combined with the cardioselective drugs AF-DX 384 and methoctramine.

The noncompetitive interactions between W84 and the various antagonists were analyzed in terms of the cooperativity model according to Christopoulos and Mitchelson (1994). Because the preceding experiments gave the values for the cooperativity of W84 with the agonist oxotremorine ($\alpha = 311$, Table 2), for the affinity of W84 at the free M_2 receptor ($K_A = 137$, Table 2), and for the affinity of the respective antagonists at the free receptor (K_B, Table 1), it was possible to estimate the degree of cooperativity between W84 and the antagonists by means of equation (2) (see Data Analysis). The resulting cooperativity factors α are listed in Table 1. It is obvious that the negative cooperativity of W84 with oxotremorine ($\alpha = 311$, Table 2) is smaller than with AF-DX 384 ($\alpha = 444$) but larger than with NMS ($\alpha = 18$) (Table 1). The equilibrium dissociation constant K_A for the binding of W84 to the free receptor does not depend on the type of ligand that is also present. Thus, the differences among the cooperativity factors for the various antagonists can be attributed to differences in the affinities of W84 at the respective antagonist/receptor complexes. According to the cooperativity model of Ehlert (1988), the affinity of an allosteric modulator to a receptor occupied by an orthosteric ligand is the product of $\alpha \cdot K_A$. These values for NMS and AF-DX 384 are shown in Table 3. If certain conditions are met, $\alpha \cdot K_A$ is equivalent to

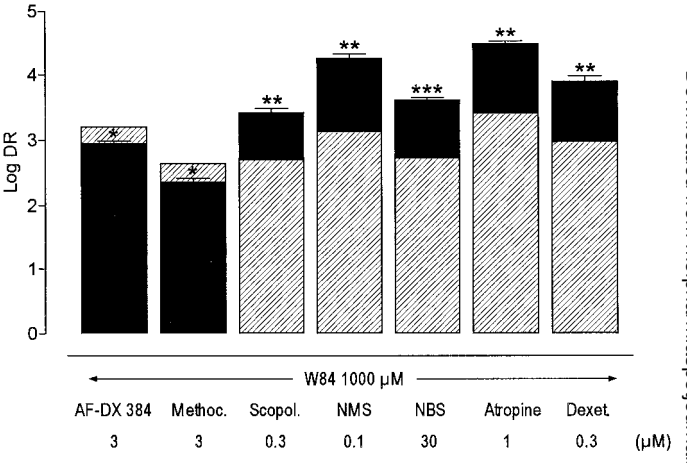

Fig. 3. Antagonistic effects induced in isolated paced guinea pig left atria by combinations of W84 (1000 μM) with the indicated antimuscarinic compounds (*Methoc.*, methoctramine; *Scopol.*, scopolamine; *Dexet.*, dexetimide). The extent of rightward shift of the oxotremorine concentration-effect curves is expressed as DR. ■, experimentally observed effects of the combinations; ▨, combination effects to be expected from the individual effects of the components if both were competitive antagonists. Results are mean values ± standard error of four to six experiments carried out in separate atrial preparations. For all combinations, the deviation between the observed and expected antagonistic effects is statistically significant (one-sample t test, two-tailed, *, $p < 0.5$; **, $p < 0.01$; ***, $p < 0.001$). In case of the combinations of W84 with AF-DX 384 and methoctramine, the effect of the combination effect was less than additive; otherwise, more-than-additive effects were induced.

TABLE 3

Synopsis of the descriptors of the allosteric interaction between W84 and the indicated ligands at guinea pig cardiac M_2 receptors, as derived from experiments in isolated atria and from radioligand binding experiments in cardiac membranes

K_A is the equilibrium dissociation constant for the binding of W84 to the unoccupied receptor, α is the cooperativity factor for the interaction of W84 with oxotremorine (Oxo), AF-DX 384, and NMS, respectively $\alpha \cdot K_A$ represents the equilibrium dissociation constant for the binding of W84 to the complex formed by the indicated ligand and the receptor, and EC_{diss} is concentration of W84 inducing a half-maximum retardation of [^{3}H]ligand dissociation.

Modulator	Oxo	AF-DX 384	NMS
W84			
Atria			
K_A (nM)	137		
α	311	444	18
$\alpha \cdot K_A$ (nM)	42,607	60,828	2,466
Membranes			
EC_{diss} (nM)		33,300	900
K_A (nM)		215	457
α		194	2.4
$\alpha \cdot K_A$ (nM)		41,700	1,097

the concentration at which the modulator induces half-maximal retardation of ligand dissociation (for details, see Lazareno and Birdsall, 1995). In other words, the $\alpha \cdot K_A$ values listed in Table 3 indicate that W84 should stabilize NMS binding to M_2 receptors with a higher potency than AF-DX 384 binding (Table 3).

To test this prediction, we measured the dissociation of [^{3}H]AF-DX 384 and [^{3}H]NMS in guinea pig cardiac membranes under the influence of W84 (Fig. 4). Under control conditions and in the presence of the test compounds, dissociation of both radioligands proceeded monophasically. The control half-life time was 4.7 ± 0.7 min (mean ± standard error; eight experiments) for [^{3}H]AF-DX 384 and 11.3 ± 0.7 min (eight experiments) for [^{3}H]NMS. W84 concentration-dependently retarded the dissociation of [^{3}H]AF-DX 384. The apparent rate constant of dissociation ($k_{-1} = \ln 2/t_{½}$) served as a measure for the rate of ligand dissociation. A plot of $100 - k_{-1}$ versus the concentration of W84 yields the concentration-response curve for the retarding action on the

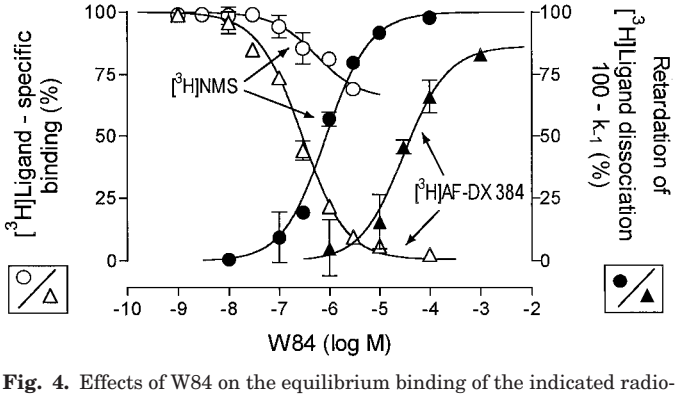

Fig. 4. Effects of W84 on the equilibrium binding of the indicated radioligands in guinea pig cardiac membranes (○, △) and on the rate of radioligand-dissociation (●, ▲). *Left ordinate*, specific binding of 2 nM [^{3}H]AF-DX 384 (△) and 0.2 nM [^{3}H]NMS (○), respectively, indicated as percentage of the control in the absence of W84. Results are mean ± standard error of three experiments, each with three replicates ([^{3}H]AF-DX 384) and two experiments each with four replicates ([^{3}H]NMS). Curve fitting was based on the ternary complex model of allosteric interactions. *Right ordinate*, retardation of the dissociation of [^{3}H]AF-DX 384 (▲) and [^{3}H]NMS (●); k_{-1} represents the apparent rate constant of dissociation as percentage of the control in the absence of W84. Results are mean ± standard error values of four independent dissociation experiments. *Scatterbars*, not shown when they do not exceed the symbols.

dissociation of [^{3}H]AF-DX 384 (Fig. 4). The curve levels off at 86%, indicating a slightly submaximal effect of W84 on [^{3}H]AF-DX 384 dissociation (partial F test, $p < 0.05$). The half-maximal effect of W84 (i.e., the inflection point of the curve) lies at $EC_{43,\ diss}$ = 33,300 nM (Table 3). In contrast, the dissociation of [^{3}H]NMS dissociation was almost completely inhibited at appropriate concentrations of W84 with the half-maximal effect attained at ~40-fold lower concentrations ($EC_{50,\ diss}$ = 900 nM; Fig. 4 and Table 3) compared with [^{3}H]AF-DX 384 as the ligand. Hill slopes were not significantly different from unity (n_H = 1.18 in the presence of the radioligand [^{3}H]AF-DX 384 and = 1.15 with [^{3}H]NMS, partial F test, $p > 0.05$).

The parameters K_A and α can be obtained from radioligand equilibrium binding experiments (Table 3) if the allosteric modulator alters equilibrium binding of the radioligand. As shown in Fig. 4, the equilibrium binding of [^{3}H]NMS was diminished only slightly by W84. The curve fit based on the cooperativity model of allosteric action (Ehlert, 1988) indicated that the bottom of the inhibition curve was located above the 50% level of specific [^{3}H]NMS binding. In contrast, W84 was capable of reducing the equilibrium binding of [^{3}H]AF-DX 384 to the zero level (Fig. 4). Because the delay of [^{3}H]AF-DX 384 dissociation requires high concentrations of W84, the inhibition curve mainly represents the inhibitive action of W84 on [^{3}H]AF-DX 384 association (i.e., the binding of W84 to the free M_2 receptor) (K_A = 215, Table 3). This value is in acceptable correspondence with the respective binding constant for W84 derived from the separate inhibition experiment with [^{3}H]NMS (K_A = 457).

At [^{3}H]NMS-occupied M_2 receptors, it was determined whether AF-DX 384 is capable of acting as an allosteric modulator by its own and whether there is an interference between the actions of W84 and AF-DX 384. AF-DX 384 retarded [^{3}H]NMS dissociation concentration-dependently (Fig. 5A). Curve fitting with a variable upper plateau did not give a better fit compared with a plateau fixed at 100% (F test, $p > 0.05$). The slope of the curve (n_H = 0.9) was not significantly different from unity (partial F test, $p > 0.05$). Half-maximal retardation of [^{3}H]NMS dissociation occurred at EC_{diss} = 22,000 nM (with n_H = 1).

To test whether AF-DX 384 interferes with the allosteric effect of W84 on the dissociation of [^{3}H]NMS, both compounds were applied in combination. To compensate for the retarding effect of AF-DX 384 on [^{3}H]NMS dissociation, the effect of the respective concentrations of AF-DX 384 alone (see also Fig. 5A) was normalized to a value of $k_{-1,\ normalized} = 1$. This procedure is equivalent to experiments previously carried out with the modulator obidoxime as allosteric "antagonist" (Tränkle and Mohr, 1997). In the presence of AF-DX 384, the allosteric delay of [^{3}H]NMS dissociation induced by 3 μM W84 was diminished concentration-dependently (Fig. 5B). The interaction of AF-DX 384 with W84 was analyzed according to Lazareno and Birdsall (1993). Because this analysis requires the control curve for the effect of W84, the curve shown in Fig. 4 for the allosteric action of W84 alone on [^{3}H]NMS dissociation is also included in Fig. 5B. Simultaneous analysis of the effector (W84) and the inhibition data (W84 plus AF-DX 384) was carried out; the slope n of the effector curve and the Schild factor s, respectively, were each checked successively for a deviation from unity. Neither n nor s deviated from unity ($p > 0.05$, data not

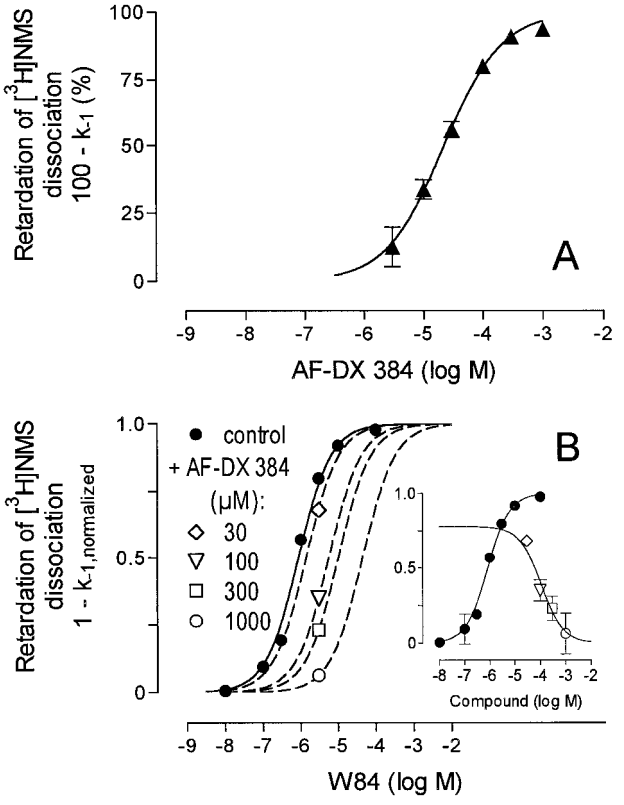

Fig. 5. Allosteric effect of AF-DX 384 on the dissociation of [^{3}H]NMS from guinea pig cardiac M_2 receptors (A) and AF-DX 384-induced attenuation of the effect of W84 on [^{3}H]NMS dissociation (B). A, *Ordinate*, retardation of [^{3}H]NMS dissociation ($100 - k_{-1}$) with k_{-1} as a percentage of the control value in the absence of AF-DX 384. *Abscissa*, log concentration of AF-DX 384. Indicated are mean values ± standard error of three to five independent experiments derived from complete dissociation curves. B, Inhibition of the retarding action of 3 μM W84 on [^{3}H]NMS dissociation by increasing concentrations of AF-DX 384 (◇, ▽, □, ○). *Ordinate*, retardation of radioligand dissociation. $k_{-1,\ \mathrm{normalized}}$ is the apparent rate constant of [^{3}H]NMS dissociation normalized to compensate for the AF-DX 384-induced delay of [^{3}H]NMS dissociation (i.e., k_{-1} observed in the presence of AF-DX 384 alone was set at $k_{-1} = 1.0$). Given are mean values of three to six data points each derived from complete dissociation curves. *Abscissa*, log concentration of W84. *Dashed curves*, parallel shift of the W84 curve elicited by increasing concentrations of AF-DX 384. *Inset*, Simultaneous nonlinear fitting of both the inhibition data and the W84 control curve was done according to Lazareno and Birdsall (1993). For the sake of clarity, experimental error (mean ± standard error) is only given in the *inset*.

shown). The Schild factor s = 1 means that the interaction of AF-DX 384 with W84 at the [^{3}H]NMS occupied receptor is compatible with a competitive mode of interaction. The pK_B value for the inhibitive action of AF-DX 384 on the allosteric effect of W84 yielded by the analysis is pK_B = 4.6 ± 0.5 (i.e., K_B = 25,000 nM). This value favorably corresponds to the $EC_{50,\ diss}$ value of 22,000 nM for the individual allosteric action of AF-DX 384 on [^{3}H]NMS dissociation. The close correspondence suggests that both effects of AF-DX 384 (i.e., inhibition of [^{3}H]NMS dissociation and antagonism of the effect of W84) are mediated via the same site of attachment on the [^{3}H]NMS-occupied M_2 receptor protein.

Discussion

In terms of the cooperativity model, W84 exerts at muscarinic M_2 receptors a negative cooperative interaction with antagonists, which, however, is considerably smaller with NMS as a representative of the nonselective antagonists ($\alpha < 20$) than with the M_2/M_4-selective antagonist AF-DX 384 ($\alpha > 190$). In principle, this difference is observed in paced guinea pig atria as well as in radioligand binding experiments (Table 3). In other words, W84 is able to inhibit the binding of AF-DX 384 to a larger extent than the binding of NMS.

The effect of an allosteric modulator on the equilibrium binding of a ligand results from the effect of the modulator on the association and on the dissociation of the ligand. The effect on the association reflects an interaction of W84 with the unoccupied receptor. W84 inhibits the association of NMS (Jepsen *et al.*, 1988) and AF-DX 384 (Fig. 4). The affinity of an allosteric modulator for the unoccupied receptor is independent of the ligand (K_A in Table 3). In contrast, the interaction of an allosteric modulator with a ligand-occupied receptor depends on the type of ligand bound to the receptor (Lee and El-Fakahany, 1988). Ligand dissociation of NMS and AF-DX 384 is impaired by W84 with largely different activity. Obviously, the affinity of W84 at the AF-DX 384-occupied receptor is lower than that for the NMS-occupied receptor; as assessed from the radioligand dissociation experiment (EC_{diss} values in Table 3), the affinity ratio is 37. The results of the independent radioligand equilibrium binding experiments ($\alpha \cdot K_A$ values in Table 3) yield an affinity ratio of 38. From the results in paced atria ($\alpha \cdot K_A$ values in Table 3), a very similar affinity ratio amounting to 25 is derived. The absolute binding affinity of W84 at the ligand-occupied receptors, however, is somewhat lower under the "physiological conditions" of the organ bath experiments compared with the radioligand binding experiments. This observation can be accounted for by the different incubation conditions with regard to temperature and ionic composition (Tränkle *et al.*, 1996).

W84 also interacts in a negative cooperative fashion with the agonists oxotremorine and arecaidine propargyl ester. The extent of the negative cooperativity with oxotremorine (α = 311, Table 3) is considerably greater than that with the antagonist NMS (α = 18). Therefore, in combination experiments, the interplay is shifted by W84 in favor of the binding of NMS compared with oxotremorine, thus inducing a more-than-additive antagonistic effect. In contrast, the degree of negative cooperativity between W84 and oxotremorine is smaller than that between W84 and AF-DX 384 (α = 444, Table 3). In other words, W84 inhibits AF-DX 384 binding more than oxotremorine binding, which explains the less-than-additive effect of this combination. A less-than-additive action was also observed for the combination of W84 with the M_2-selective antagonist methoctramine but not with any of the other antagonists. The latter compounds are structurally heterogeneous, but they share a nonselective behavior. This coincidence suggests a relationship between the low affinity of W84 for the AF-DX 384-occupied receptor and the special binding mode of this M_2-preferring antagonist.

On the molecular level, there are two possible explanations for the low affinity of W84 at the AF-DX 384-occupied M_2 receptor. First, AF-DX 384 may stabilize the M_2 receptor in another conformation than does NMS, and the conformation induced or stabilized by AF-DX 384 may have a low affinity for W84. Second, the receptor protein may have the same conformation with bound AF-DX 384 as with bound NMS, but AF-DX 384 imposes a steric hindrance for the attachment

of W84, thus allowing only part of the W84 molecule to bind. This hypothesis is illustrated in Fig. 6. Because AF-DX 384 affects receptor G protein coupling with negative intrinsic activity, as does the tropate atropine (Hilf and Jakobs, 1992), it seems reasonable to assume that AF-DX 384 and the tropate NMS stabilize the receptor in the same conformation. AF-DX 384 may bind in a way that it uses part of the allosteric site. This notion is supported by the results of Kerckhoff and Höltje (1994), who used a conformational analysis and receptor modeling approach for various M_2- and M_1-selective derivatives of pirenzepine to assess the orientation of the compounds in the ligand binding pocket of the receptor protein. It seemed pivotal for the M_2 receptor binding of AF-DX 116, which is a close congener of AF-DX 384, that the side chain is directed toward the entrance of the ligand binding pocket. As noted above, the allosteric site is likely to be located in this region of the M_2 receptor. According to a recent structure-activity relationship study, the W84 molecule in its entire length is involved in the binding to the allosteric site of [^{3}H]NMS-occupied M_2 receptors (Kostenis *et al.*, 1994). Shared points of attachment between AF-DX 384 and W84 would explain why the affinity of W84 at the AF-DX 384-occupied receptor compared with the NMS-occupied receptor is reduced.

In this context, the findings of Christopoulos and Mitchelson (1994) should be mentioned; they applied the heptamethonium analogue of W84 (i.e., heptane-1,7-bis(dimethyl-3′-phthalimidopropyl) ammonium bromide) in combination with NMS and with the M_1-selective antagonist pirenzepine in paced guinea pig atria. Pirenzepine has the same tricyclic backbone as AF-DX 384 and AF-DX 116 but differs in the nature of the side chain and the spatial location of the protonated nitrogen (Eberlein *et al.*, 1989). Combinations of C_7/3′-phth with pirenzepine still acted supra-additively, but the extent of supra-additivity was considerably less pronounced than that in combinations of C_7/3′-phth with NMS. Remarkably, Kerckhoff and Höltje (1994) suggested that pirenzepine attaches to the M_2 receptor in the same orientation as AF-DX 116 (i.e., with the nitrogen directed toward the entrance of the ligand binding pore). For pirenzepine, however, this is an unfavorable position leading to a low binding affinity at the M_2 receptor. This low affinity precludes direct binding experiments with radiolabeled pirenzepine to study further the interaction with the allosteric modulator C_7/3′-phth. However, having in mind the high negative cooperativity between C_7/3′-phth and pirenzepine (α = 58) compared with NMS (α = 9), as reported by Christopoulos and Mitchelson (1994), it is tempting to assume that pirenzepine interferes with the binding of C_7/3′-phth to the allosteric site in a similar way as proposed here for the respective analogues AF-DX 384 and W84.

As found with other M_2-preferring compounds such as AF-DX 116 (Lee and El-Fakahany, 1991), AF-DX 384 is capable of stabilizing NMS receptor complexes. This effect may result from an interaction with the allosteric binding site in [^{3}H]NMS-occupied M_2 receptors as illustrated in Fig. 6. This idea is compatible with the lower affinity of AF-DX 384 at the [^{3}H]NMS-occupied receptor (EC_{diss} = 22,000 nM) compared with the free M_2 receptor (K_D = 11 nM). In the first case, NMS hinders the ring system of AF-DX 384 from binding. In the latter case, the docking place for the ring system is available, allowing for a pronounced gain in affinity. As far as [^{3}H]NMS-occupied receptors are concerned, the binding affinity of AF-DX 384 is much lower than that of W84 (EC_{diss} = 22,000 versus 900 nM) yet similar to the affinity of the prototype modulator gallamine (EC_{diss} = 16,000 nM, Tränkle *et al.*, 1996). The character of the interaction between W84 and AF-DX 384 at the NMS-occupied receptor is formally competitive (Fig. 5). This finding suggests that AF-DX 384 interacts with the common allosteric site of NMS-occupied M_2 receptors (Ellis and Seidenberg, 1992; Tränkle and Mohr, 1997). Yet, we are aware that it is speculative to assume that the part of AF-DX 384 that is capable of attaching to the NMS-occupied receptor is identical with the part of the molecule that possibly binds to the allosteric site when AF-DX 384 attaches to the free receptor.

With regard to the interaction of methoctramine with M_2 receptors, Melchiorre *et al.* (1989) proposed that the binding domain of this long tetraamine molecule includes the orthosteric and the allosteric recognition site of the receptor protein. This hypothesis is supported by our finding that methoctramine like AF-DX 384 is less-than-additive anti-

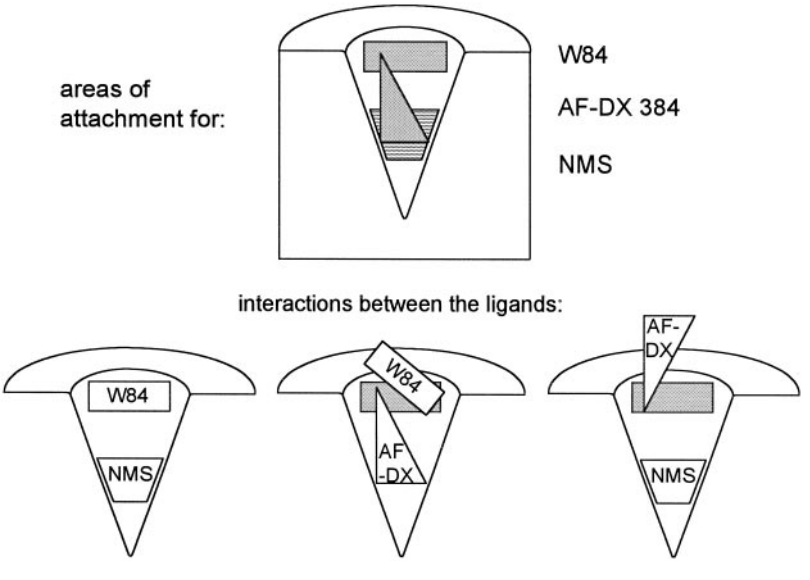

Fig. 6. Sketch of a tentative explanation of the experimental findings. *Top*, test compounds occupy differing areas of attachment at the ligand binding pore of the receptor protein. *Bottom left*, with the orthosteric site occupied by NMS, W84 in its whole length may bind to the allosteric site of the receptor protein and thus prevent the dissociation of NMS (cf. to the model of Proška and Tuček, 1994). *Bottom middle*, with AF-DX 384 bound, part of the allosteric site is occupied by this antagonist. Thus, only part of the allosteric site remains available for W84; consequently, its binding affinity and its potency to retard radioligand dissociation are lower at the AF-DX 384/receptor complexes compared with NMS/receptor complexes. *Bottom right*, with NMS bound to the receptor, part of the AF-DX 384 molecule attaches to the allosteric site allowing only for a moderate binding affinity compared with AF-DX 384 binding to the free receptors; at appropriate concentrations, AF-DX 384 may, thus, inhibit the dissociation of NMS.

muscarinic in combination with W84 (Fig. 3). Furthermore, methoctramine is known to interact with [^{3}H]NMS-occupied M_2 receptors having a 7-fold higher affinity ($EC_{50,\ diss}$ = 3,000 nM; Tränkle *et al.*, 1996) than AF-DX 384 ($EC_{50,\ diss}$ = 22,000 nM). Thus, methoctramine and AF-DX 384 seem to interact with M_2 receptors in a similar fashion.

In conclusion, the results presented here suggest "shared points of attachment" between the muscarinic antagonist AF-DX 384 and the potent allosteric modulator W84. It is tempting to assume that M_2-preferring antagonists may derive part of their receptor subtype selectivity from an interaction with the common allosteric site of the M_2 receptor protein.

Acknowledgments

We gratefully acknowledge the excellent technical assistance of Micheline Neubert (Kiel, Germany) and Frauke Mörschel and Iris Witten (Bonn, Germany).

References

Arunlakshana O and Schild HO (1959) Some quantitative uses of drug antagonists. *Br J Pharmacol* **14:**48–58.
Birdsall NJM, Chan SC, Eveleigh P, Hulme EC, and Miller KW (1989) The modes of binding of ligands to cardiac muscarinic receptors. *Trends Pharmacol Sci* **10**(suppl.)**:**31–34.
Christopoulos A and Mitchelson F (1994) Assessment of the allosteric interactions of the bisquaternary heptane-1,7-bis(dimethyl-3′-phthalimido-propyl)ammonium bromide at M_1 and M_2 muscarine receptors. *Mol Pharmacol* **46:**105–114.
Clark AL and Mitchelson F (1976) The inhibitory effect of gallamine on muscarinic receptors. *Br J Pharmacol* **58:**323–331.
DeBlasi A, O′Reilly K, and Motulsky HJ (1989) Calculating receptor number from binding experiments using same compound as radioligand and competitor. *Trends Pharmacol Sci* **10:**227–229.
Eberlein WG, Engel W, Mihm G, Rudolf K, Wetzel B, Entzeroth M, Mayer N, and Doods HN (1989) Structure-activity relationships and pharmacological profile of selective tricyclic antimuscarinics. *Trends Pharmacol Sci* **10**(suppl.)**:**50–54.
Ehlert FJ (1988) Estimation of the affinities of allosteric ligands using radioligand binding and pharmacological null methods. *Mol Pharmacol* **35:**187–194.
Ellis J and Seidenberg M (1992) Two allosteric modulators interact at a common site on cardiac muscarinic receptors. *Mol Pharmacol* **42:**638–641.
Ellis J, Huyler J, and Brann MR (1991) Allosteric regulation of cloned m1–m5 muscarinic receptor subtypes. *Biochem Pharmacol* **42:**1927–1932.
Ellis J, Seidenberg M, and Brann MR (1993) Use of chimeric muscarinic receptors to investigate epitopes involved in allosteric interactions. *Mol Pharmacol* **44:**583–588.
Entzeroth M and Mayer N (1990) Labeling of rat heart muscarinic receptors using the new M_2 selective antagonist [^{3}H]AF-DX 384. *Biochem Pharmacol* **40:**1674–1676.
Hilf G and Jakobs KH (1992) Agonist-independent inhibition of G protein activation by muscarinic acetylcholine receptor antagonists in cardiac membranes. *Eur J Pharmacol* **225:**245–252.
Jakubík J and Tuček S (1995) Positive interactions on cardiac muscarinic receptors: effect of chemical modifications of disulphide and carboxyl groups. *Eur J Pharmacol* **289:**311–319.
Jakubík J, Bačáková L, El-Fakahany EE, and Tuček S (1995) Subtype selectivity of the positive allosteric action of alcuronium at cloned M_1-M_5 muscarinic receptor subtypes. *J Pharmacol Exp Ther* **274:**1077–1083.
Jepsen K, Lüllmann H, Mohr K, and Pfeffer J (1988) Allosteric stabilisation of [^{3}H]-*N*-methylscopolamine binding in guinea pig myocardium by an antidote against organophosphate intoxication. *Pharmacol Toxicol* **63:**163–168.
Kerckhoff H and Höltje HD (1994) Conformational analysis and receptor modelling of m1 and m2 selective antagonists. *Pharmazie* **49:**566–573.
Kostenis E and Mohr K (1996) Composite action of allosteric modulators on ligand binding (letter reply). *Trends Pharmacol Sci* **17:**443–444.
Kostenis E, Holzgrabe U, and Mohr K (1994) Allosteric effect on muscarinic M_2-receptors of derivatives of the alkane-bis-ammonium compound W84: comparison with bispyridinium-type allosteric modulators. *Eur J Med Chem* **29:**947–953.
Lanzafame A, Christopoulos A, and Mitchelson F (1996) Interactions of agonists with an allosteric antagonist at muscarinic acetylcholine M_2 receptors. *Eur J Pharmacol* **316:**27–32.
Lazareno S and Birdsall NJM (1993) Estimation of competitive antagonist affinity from functional inhibition curves using the Gaddum, Schild and Cheng-Prusoff equations. *Br J Pharmacol* **109:**1110–1119.
Lazareno S and Birdsall NJM (1995) Detection, quantitation, and verification of allosteric interactions of agents with labeled and unlabeled ligands at G protein-coupled receptors: interaction of strychnine and acetylcholine at muscarinic receptors. *Mol Pharmacol* **48:**362–378.
Lee NH and El-Fakahany EE (1988) Influence of ligand choice on the apparent binding profile of gallamine to cardiac muscarinic receptors: identification of three main types of gallamine-muscarinic receptor interaction. *J Pharmacol Exp Ther* **246:**829–838.
Lee NH and El-Fakahany EE (1991) Allosteric interactions at the m_1, m_2 and m_3 muscarinic receptor subtypes. *J Pharmacol Exp Ther* **256:**468–479.
Leppik RA, Miller RC, Eck M, and Paquet JL (1994) Role of acidic amino acids in the allosteric modulation by gallamine of antagonist binding at the m_2 muscarinic acetylcholine receptor. *Mol Pharmacol* **45:**983–990.
Lüllmann H, Ohnesorge FK, Schauwecker GC, and Wassermann O (1969) Inhibition of the actions of carbachol and DFP on guinea pig isolated atria by alkane-bis-ammonium compounds. *Eur J Pharmacol* **6:**241–247.
Lüβ H and Mohr K (1992) Comparison between the stabilizing effects of W84 on [^{3}H]NMS-binding in cardiac membranes and in beating atria from guinea pig hearts. *Naunyn-Schmiedeberg's Arch Pharmacol* **345:**R101.
Maaβ A, Kostenis E, and Mohr K (1995) Potentiation by alcuronium of the antimuscarinic effect of N-methylscopolamine in guinea pig left atria. *Eur J Pharmacol* **272:**103–106.
Melchiorre C, Minarini A, Angeli P, Giardina D, Gulini U, and Quaglia W (1989) Polymethylene tetramines as muscarinic receptor probes. *Trends Pharmacol Sci* **4**(suppl.)**:**50–54.
Miller JH, Gibson VA, and McKinney M (1991) Binding of [^{3}H]AF-DX 384 to cloned and native muscarinic receptors. *J Pharmacol Exp Ther* **259:**601–607.
Pedder EK, Eveleigh P, Poyner D, Hulme EC, and Birdsall NJM (1991) Modulation of the structure-binding relationships of antagonists for muscarinic acetylcholine receptor subtypes. *Br J Pharmacol* **103:**1561–1567.
Proška J and Tuček S (1994) Mechanisms of steric and cooperative actions of alcuronium on cardiac muscarinic acetylcholine receptors. *Mol Pharmacol* **45:**709–717.
Tränkle C and Mohr K (1997) Divergent modes of action among cationic allosteric modulators of muscarinic M_2 receptors. *Mol Pharmacol* **51:**674–682.
Tränkle C, Kostenis E, Burgmer U, and Mohr K (1996) Search for lead structures to develop new allosteric modulators of muscarinic receptors. *J Pharmacol Exp Ther* **279:**926–933.
Trumpp-Kallmeyer S, Hoflack J, Bruinvels A, and Hibert M (1992) Modeling of G-protein-coupled receptors: application to dopamine, adrenaline, serotonin, acetylcholine, and mammalian opsin receptors. *J Med Chem* **35:**3448–3462.
Waelbroeck M, Camus J, Tastenoy M, Feifel R, Mutschler E, Tacke R, Strohmann C, Rafeiner K, Rodrigues de Miranda JF, and Lambrecht G (1994) Binding and functional properties of hexocyclium and sila-hexocyclium derivatives to muscarinic receptor subtypes. *Br J Pharmacol* **112:**505–514.
Waelbroeck M, Lazareno S, Pfaff O, Friebe T, Tastenoy M, Mutschler E, and Lambrecht G (1996) Stereoselective recognition of the enantiomers of phenylglutarimide and of six related compounds by four muscarinic receptor subtypes. *Br J Pharmacol* **119:**1319–1330.
Wassermann O (1970) Untersuchungen zur Pharmakokinetik bis-quartärer Substanzen in vivo und in vitro. Ph.D. dissertation, University of Kiel, Kiel, Germany.
Wess J (1993) Molecular basis of muscarinic acetylcholine receptor function. *Trends Pharmacol Sci* **14:**308–313.
Wess J, Gdula D, and Brann MR (1992) Structural basis of the subtype selectivity of muscarinic antagonists: a study with chimeric m2/m5 muscarinic receptors. *Mol Pharmacol* **41:**369–374.
Wheatley M, Hulme EC, Birdsall NJM, Curtis CAM, Eveleigh P, Pedder EK, and Poyner D (1988) Peptide mapping studies on muscarinic receptors: receptor structure and location of the ligand binding site. *Trends Pharmacol Sci* **9**(suppl.)**:**19–24.

Send reprint requests to: Klaus Mohr, Pharmacology & Toxicology, Institute of Pharmacy, University of Bonn, An der Immenburg 4, 53121 Bonn, Germany. E-mail: k.mohr@uni-bonn.de